Acta Crystallographica Section D
Biological Crystallography
ISSN 0907-4449

Flash-cooling and annealing of protein crystals

S. Kriminski,[a] C. L. Caylor,[a] M. C. Nonato,[b] K. D. Finkelstein[c] and R. E. Thorne[a]*

[a]Laboratory of Atomic and Solid State Physics, Cornell University, Ithaca, NY 14853, USA, [b]Department of Chemistry and Chemical Biology, Cornell University, Ithaca, NY 14853, USA, and [c]Cornell High-Energy Synchrotron Source (CHESS), Ithaca, NY 14853, USA

Correspondence e-mail: ret6@cornell.edu

Received 6 August 2001
Accepted 2 January 2002

Flash-cooling and annealing of macromolecular crystals have been investigated using *in situ* X-ray imaging, diffraction-peak lineshape measurements and conventional crystallographic diffraction. The dominant mechanisms by which flash-cooling creates disorder are suggested and a fixed-temperature annealing protocol for reducing this disorder is demonstrated that should be more reliable and flexible than existing protocols. Flash-cooling tetragonal lysozyme crystals degrades diffraction resolution and broadens the distributions of lattice orientations (mosaicity) and lattice spacings. The diffraction resolution strongly correlates with the width of the lattice-spacing distribution. Annealing at fixed temperatures of 253 and 233 K consistently reduces the lattice-spacing spread and improves the resolution for annealing times up to ∼30 s. X-ray images show that this improvement arises from the formation of well ordered domains with characteristic sizes >10 μm and narrower mosaicities than the crystal as a whole. Flash-cooled triclinic crystals of lysozyme, which have a smaller water content than the tetragonal form, diffract to higher resolution with smaller mosaicities and exhibit pronounced ordered domain structure even before annealing. It is suggested that differential thermal expansion of the protein lattice and solvent may be the primary cause of flash-cooling-induced disorder. Mechanisms by which annealing at $T << 273$ K reduce this disorder are discussed.

1. Introduction

Cryocrystallographic techniques are now widely used for X-ray data collection in structure determination of biological macromolecules. Flash-cooling macromolecular crystals to $T \leq 150$ K reduces radiation damage and increases crystal lifetimes in intense X-ray beams by a factor of $\sim 10^3$, in favorable cases allowing complete diffraction data sets to be collected using a single crystal (Hope, 1988, 1990; Young *et al.*, 1993; Rodgers, 1994; Watowich *et al.*, 1995; Chayen *et al.*, 1996; Garman & Schneider, 1997; Garman, 1999). Flash-cooling can also decrease background scattering and reduce atomic B factors (Singh *et al.*, 1980; Young *et al.*, 1994).

However, cryogenic data collection has its costs. Well faceted macromolecular crystals having room-temperature diffraction resolutions suitable for structure determinations generally have extremely narrow mosaic widths (<0.02°) and the mosaicity parameter extracted using diffraction analysis programs is almost always determined by the characteristics of the experimental setup, *e.g.* the incident beam divergence (Dobrianov *et al.*, 1999; Nave, 1999). They also exhibit little or no strain, with a typical lattice-spacing distribution of <0.05% (Dobrianov *et al.*, 1998). However, when these crystals are

flash-cooled, the crystal mosaicity can broaden to 0.2° or more, indicating the presence of substantial lattice orientational disorder. Diffraction resolution also degrades, sometimes dramatically. Flash-cooling-induced disorder thus reduces the accuracy of electron-density maps and molecular structures. This may be especially true at third generation synchrotron sources where the broad mosaicities limit signal-to-noise improvements made possible by the small beam divergence.

One of the most interesting and potentially important discoveries in recent years is that diffraction properties of flash-cooled macromolecular crystals can often be improved by warming and then cooling a second time. Two different crystal-annealing protocols have been reported (Harp *et al.*, 1998, 1999; Yeh & Hol, 1998; Garman, 1999; Samygina *et al.*, 2000) and many variants of these have been tried in the field. In the first, a flash-cooled crystal is removed from the cold gas stream, placed in a cryoprotectant solution for 3 min and then recooled (Harp *et al.*, 1998, 1999). In the second, the cold stream is blocked for a fixed time or until signs of melting become visible, and the crystal is then recooled (Yeh & Hol, 1998). Both annealing protocols can improve crystal resolution and mosaicity, although substantial crystal-to-crystal and molecule-to-molecule variability has been observed. Annealing cannot restore crystals and diffraction to their pre-cooling as-grown quality, but the full extent of improvement possible has not been systematically explored.

Here, we describe *in situ* studies of flash-cooling-induced disorder and annealing using tetragonal and triclinic crystals of hen egg-white lysozyme. Flash-cooling introduces large lattice stresses that produce short-length-scale disorder responsible for mosaic broadening and resolution degradation. Annealing crystals at fixed temperatures between 253 and 233 K causes release of lattice stresses and leads to formation of larger, better ordered domains. We suggest that differential thermal expansion of the protein lattice and solvent during flash-cooling is largely responsible for the observed disordered microstructure, and discuss mechanisms by which annealing reduces this disorder.

2. Materials and methods

Although exceptionally easy to grow, the crystal polymorphs of lysozyme show a range of flash-cooling behaviors and thus provide reasonable models for flash-cooling and annealing studies. Tetragonal hen egg-white lysozyme (HEWL) crystals were grown in agarose gels [0.1%(*w*/*v*)] at T = 294 K from solutions consisting of 40–60 mg ml^{-1} lysozyme (Seikagaku, 6× recrystallized) and 0.5 *M* NaCl in 50 m*M* acetate buffer pH 4.5. Gel growth yields extremely high-quality crack-free crystals with very small mosaicities (<0.005°, similar to Si monochromator crystals). This high initial perfection allows flash-cooling-induced disorder to be easily detected. Gel-grown crystals also have essentially perfect symmetrical habits with well defined facets, unlike the irregular crystals produced in hanging or sitting drops as a result of crystal truncation at the liquid–vapor and liquid–cover slip interfaces. Consequently, gel-grown crystals should flash-cool more symmetrically, allowing shape effects to be separated from intrinsic behavior. High-quality triclinic lysozyme crystals with mosaicities of <0.01° were grown by the hanging-drop method at T = 294 K without gels from solutions consisting of 14 mg ml^{-1} lysozyme and 0.25 *M* $NaNO_3$ in 50 m*M* acetate buffer pH 4.5.

The tetragonal and triclinic crystal forms of lysozyme contain ∼42 and ∼26%(*w*/*w*) water, respectively, and triclinic lysozyme survives flash-cooling much better. All experiments used relatively large crystals of typical size ∼0.7 mm, in part because successful flash-cooling of larger crystals is generally more difficult. Larger crystals also have smaller surface-to-volume ratios, so that stresses associated with flash-cooling of any residual surrounding liquid should be less important, allowing intrinsic behavior of the crystal itself to be determined.

Crystals were transferred from the mother liquor to Paratone N oil, mounted in CryoLoops (Hampton Research) and then flash-cooled by immersion in liquid nitrogen. Paratone oil was used to remove external water and eliminate associated ice rings. Additional penetrating cryoprotectants were not used since we chose to focus these initial investigations on the behavior of as-grown crystals. CryoLoop sizes were smaller than the crystal size to minimize excess oil.

Experiments were performed at the Cornell High-Energy Synchrotron Source (CHESS) using a Molecular Structure Corporation heat-exchanging nitrogen-flow cryocooler. Lysozyme samples were mounted on a magnetic goniometer head by rapid transfer from liquid nitrogen into the cold nitrogen stream using a CryoTong (Hampton Research), following standard procedures (Hope, 1990; Rodgers, 1994; Young *et al.*, 1994; Kurinov & Harrison, 1995; Garman & Schneider, 1997; Parkin & Hope, 1998; Garman, 1999). Flow temperatures were 150 K. Measurements of liquid-nitrogen flash-cooled crystals at temperatures between 100 and 200 K using a laboratory X-ray source showed that the diffraction properties did not degrade during several hours at 150 K. At this temperature Young's modulus and other crystal mechanical properties are nearly temperature independent (Morozov & Gevorkian, 1985) and appreciable relaxation of amorphous ice to crystalline ice does not occur on the 30–120 min timescale of our experiments (Miyazaki *et al.*, 2000).

Two different *in situ* annealing protocols were used. In the first, crystals were annealed by diverting the cold nitrogen stream for 5–10 s or until sample changes indicating impending melting were observed as in 'flash-annealing' (Yeh & Hol, 1998). In the second, the temperature of the cryostream, monitored using a type K thermocouple placed ∼0.5 cm above the sample, was abruptly changed and then maintained at a nearly constant value by dynamically adjusting the mix of cold and warm gas. Flow temperatures could be changed from 150 to 250 ± 2 K in ∼5–10 s. Crystal temperature equilibration with the flow occurs on a comparable timescale (Teng & Moffat, 1998; Walker *et al.*, 1998). Although more reproducible than the flash-annealing protocol, uncertainties in this temperature-controlled annealing arose from irreproducibilities in the actual warming

and recooling rates and from temperature fluctuations during annealing.

X-ray data collection on CHESS materials science stations F-3 and C-1 used unfocused 1.24 Å X-rays selected by Si[111] double-bounce monochromators. Partial crystallographic data sets (typically three 2° oscillations or, for crystals with large post-cooling rocking widths, six stationary patterns covering 8°) were collected using image plates and analyzed using *DENZO* and *SCALEPACK*. Because of the variety of diffraction measurements to be performed, experimental setups were not optimized for collecting image-plate data. Measured diffraction resolutions were thus at least 0.4 Å lower than those obtained using similar-quality crystals on crystallography beamlines.

Diffraction-peak lineshape measurements were performed on station C-1 using a six-circle diffractometer. The incident beam energy spread and vertical divergence were $\Delta E/E \simeq 2 \times 10^{-4}$ and 4×10^{-5} rad, respectively. Mosaic (ω) scans were performed by fixing the detector and rotating the crystal about the axis normal to the scattering plane. In reciprocal space these scans are normal to the scattering wavevector **Q** and measure the distribution of lattice orientations within the crystal. Radial or ω–2θ scans along the scattering wavevector **Q**, performed by rotating the crystal and detector together, measure the distribution of lattice spacings (strain). An Si[111] analyzer crystal on the 2θ arm provided an angular resolution $\Delta(2\theta) \simeq 0.003°$. However, 2θ widths for flash-cooled crystals were typically one to two orders of magnitude larger than this resolution. To improve throughput, in most mosaic and ω–2θ measurements the angular acceptance of the detector was instead defined by vertical slits as $\Delta(2\theta) \simeq 0.02°$. Lineshape measurements were performed near $2\theta = 12°$, corresponding to a diffraction resolution $d = \lambda/(2\sin\theta)$ of 6 Å.

X-ray topography measurements (Tanner, 1976; Fourme *et al.*, 1995; Izumi *et al.*, 1996; Stojanoff & Siddons, 1996; Dobrianov *et al.*, 1998, 1999, 2001; Otalora *et al.*, 1999; Vidal *et al.*, 1999) were performed on station F-3 by illuminating the entire crystal using a highly parallel (unfocused) monochromatic X-ray beam and recording the diffraction pattern using fine-grain high spatial resolution film (Kodak Industrex SR) placed ∼5 cm from the sample. Under these illumination and detection conditions, every Bragg spot is a unit magnification image of the crystal. Image contrast arises from variations in the strength of diffraction from point to point within the crystal bulk associated with variations in lattice orientation, spacing and overall order. This imaging technique is ideally suited to studying flash-cooling-induced disorder because it can be applied *in situ* and is sensitive to the kinds of bulk disorder that matter in crystallography. The horizontal and vertical beam divergences were $\sim 1 \times 10^{-3}$ and 3×10^{-5} rad, respectively, measured by comparing images of the direct beam at various distances from defining slits. The image resolution was a few micrometres.

Diffraction patterns, lineshape measurements and/or X-ray topographs were collected from a total of 23 tetragonal lysozyme crystals and three triclinic lysozyme crystals. As is evident from previous work and as discussed later, annealing has the greatest benefits for crystals that suffer the greatest damage during flash-cooling. Consequently, results for both well frozen and poorly frozen crystals will be described.

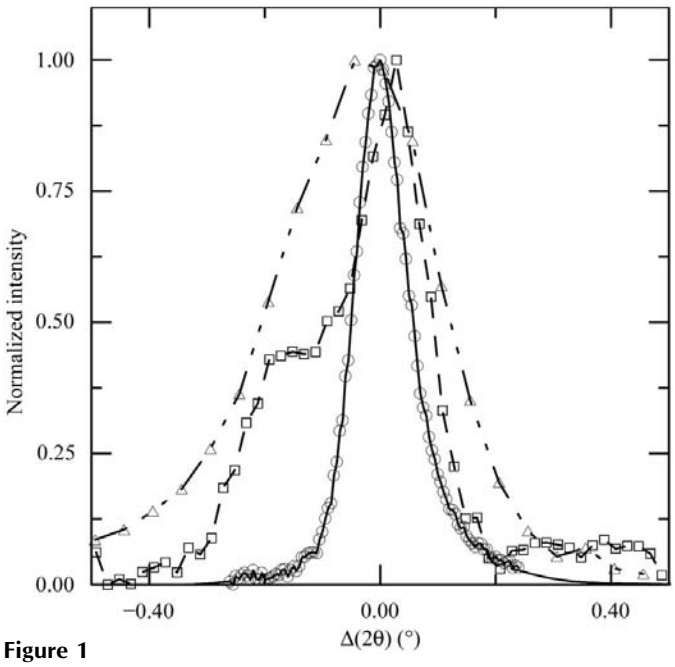

Figure 1
Examples of ω–2θ scans for flash-cooled tetragonal lysozyme crystals, acquired near $2\theta \simeq 12°$ or a resolution of ≃6 Å. The full-width-at-half-maximum values (FWHMs) are ∼0.35, 0.2 and 0.1° for samples represented by triangles, squares and crosses, respectively. The corresponding diffraction resolutions at $I/\sigma = 8$ are 2.9, 2.5 and 1.8 Å, respectively.

3. Experimental results

3.1. Tetragonal lysozyme: flash-cooling

Flash-cooling tetragonal lysozyme crystals degraded their mosaicity and diffraction resolution. Typical mosaic full-width-at-half-maximum (FWHM) values before flash-cooling are instrumentally limited (≤0.005°) and typical diffraction resolutions obtained with our experimental setup are ∼1.6 Å for $I/\sigma = 8$. After flash-cooling, mosaic FWHM values for our relatively large crystals broadened to ∼0.5–1.5° and resolution for $I/\sigma = 8$ increased to 2.6 ± 0.5 Å.

Fig. 1 shows ω–2θ scans through diffraction peaks near $2\theta = 12°$ for three flash-cooled tetragonal lysozyme crystals. Measurements before flash-cooling yield instrumentally limited 2θ FWHMs of ∼0.003° (Dobrianov *et al.*, 1998; Caylor *et al.*, 1999), corresponding to a lattice-constant spread within the crystal of less than 0.03%. This implies that as-grown crystals are not appreciably strained. FWHMs of flash-cooled crystals were ∼0.2° and correspond to a spread in lattice spacings of ∼2%. The diffraction peaks for as-grown crystals are symmetric and have narrow tails, whereas the peaks for flash-cooled crystals can be more structured and show broad tails.

The post-flash-cooling width of the lattice-constant distribution and thus the extent to which the lattice is strained strongly correlate with the diffraction resolution. For example, crystals with 2θ widths of 0.2 and 0.12° diffracted to resolutions of 2.9 and 1.9 Å, respectively. This suggests that lattice stresses associated with non-uniform lattice contraction during flash-cooling play an important role in degrading resolution and mosaicity. Our 2θ widths are consistent with estimates of 0.1–0.25° for flash-cooled tetragonal lysozyme crystals obtained from analysis of diffraction spot shapes (Nave, 1998). Our mosaic widths were significantly larger than the 2θ widths, so that the mosaicity parameter was dominated by lattice orientational disorder rather than by strain.

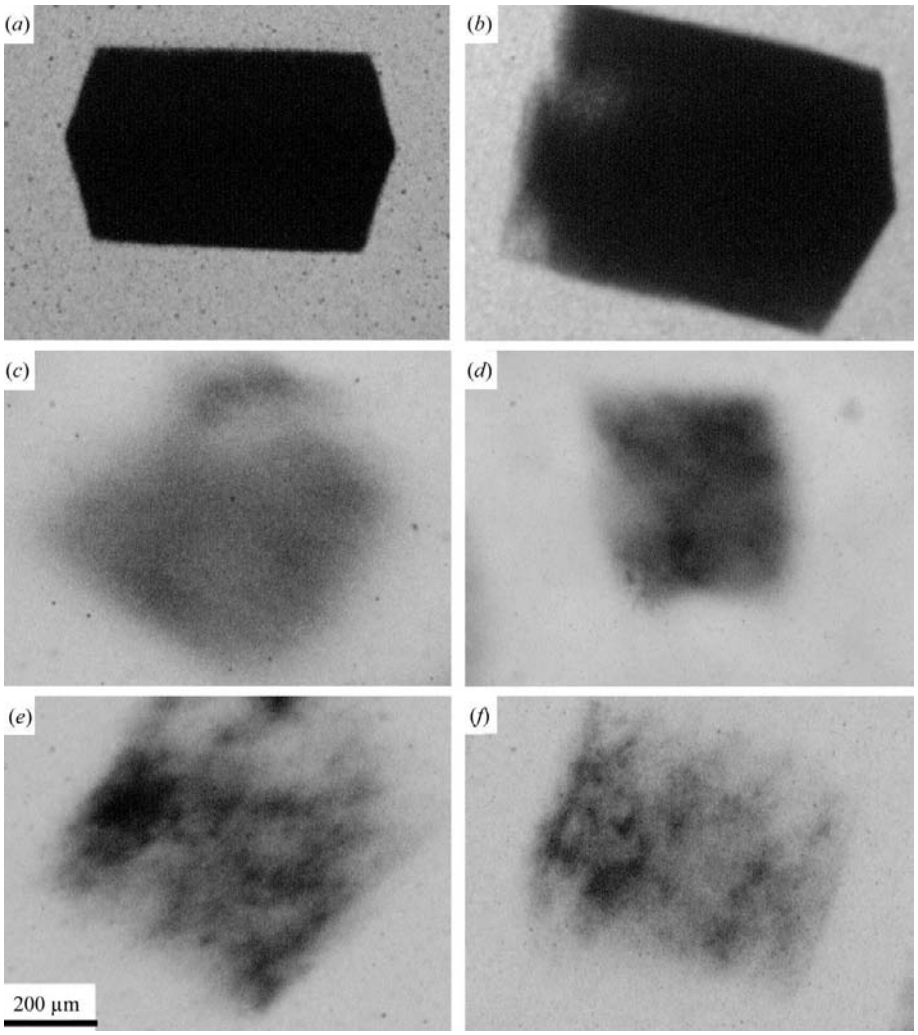

Figure 2
X-ray images of (*a* and *b*) native gel-grown tetragonal HEWL crystals and (*c* and *d*) flash-cooled gel-grown tetragonal HEWL crystals. (*e*) Crystal in (*c*) after 6 s 'flash' annealing. The diffraction resolution at $I/\sigma = 8$ has improved from 2.5 to 2.0 Å. (*f*) Crystal in (*d*) after a 25 s annealing at 250 K. The crystal in (*d*) was poorly handled during flash-cooling and the diffraction resolution improved from 4.3 to 2.4 Å.

Fig. 2 shows typical X-ray images of tetragonal lysozyme crystals acquired before (Figs. 2*a* and 2*b*) and after (Figs. 2*c* and 2*d*) flash-cooling. Images acquired before flash-cooling show little contrast aside from gradual intensity variations owing to crystal bending. Flash-cooled crystals show smooth intensity variations but no sharp contrast that would indicate the presence of cracks (which, for example, produce strong contrast and broad mosaic widths in crystals with non-uniform impurity distributions; Caylor *et al.*, 1999) or of other less severe defects such as dislocations. Given their broad mosaic and 2θ widths, this indicates that the crystals have densities of dislocations and other microscopic defects that are too large to allow individual defects to be resolved. This differs from the strong contrast from dislocations and other defects observed in far less disordered lysozyme crystals grown, for example, by macroseeding (Dobrianov *et al.*, 1998). The images in Figs. 2(*c*) and 2(*d*) appear smeared out and are larger than would be expected

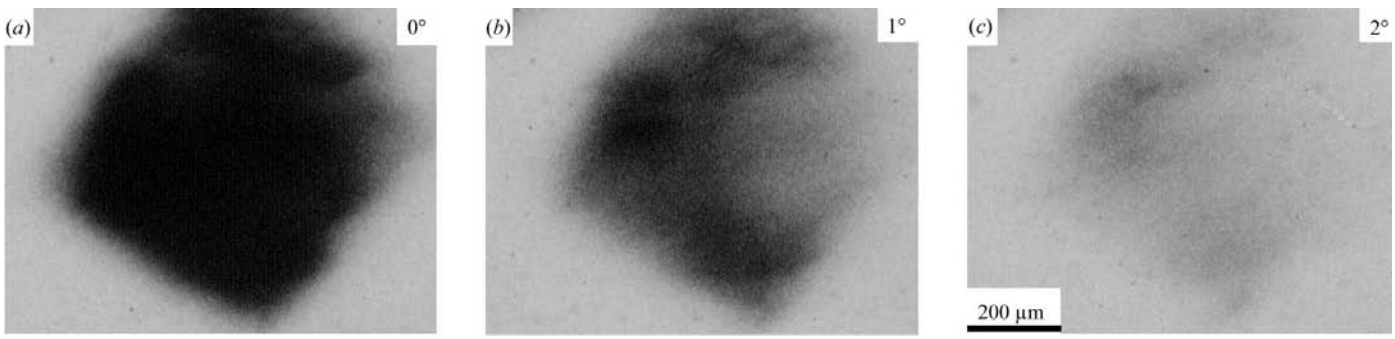

Figure 3
Sequence of X-ray images for a flash-cooled gel-grown tetragonal HEWL crystal acquired at successive angles in the rocking curve of the reflection used to form the image. The crystal's diffraction resolution at $I/\sigma = 8$ is 2.7 Å.

based on the incident X-ray beam divergence and the crystal size. This implies that the diffracted beam has a larger angular divergence than the incident beam and that there is a large spread in lattice spacings within the crystal. The 2θ divergence estimated from the image smearing is $\sim$0.1–0.2°, consistent with that obtained by direct measurements as in Fig. 1. Flash-cooled crystals do not show structured contrast corresponding to variations in local rocking width or peak position on the scale of the crystal size that would indicate damage from the surrounding oil or from handling, so that the origin of the observed disorder is primarily internal to the crystal.

Fig. 3 shows X-ray images of a flash-cooled crystal acquired at successive angles within the $\sim$2° wide rocking curve of the reflection used for the image. As the crystal is rocked off the diffraction peak, the diffracted intensity fades out more or less uniformly over the crystal. This implies that the rocking width of any small piece of the crystal is comparable to the rocking width of the overall crystal, an example of 'microscopic' mosaicity (Dobrianov *et al.*, 1998). In other words, the lattice orientational disorder responsible for the broad rocking width and mosaicity occurs on shorter length scales than can be resolved in our images (a few micrometres) and appears to be more or less uniformly distributed within the crystal.

3.2. Tetragonal lysozyme: annealing

Annealing at fixed temperatures of T = 250 and 230 K significantly improved the resolution of nearly all crystals, with poorly diffracting crystals showing the largest improvements. For crystals that initially diffracted in the range 2.6 $\pm$ 0.5 Å (at I/σ = 8), resolution improved to 2.3 $\pm$ 0.3 Å. For crystals that were poorly handled during flash-cooling that initially diffracted in the range 3.7 $\pm$ 0.5 Å, resolution improved to 2.3 $\pm$ 0.3 Å. The common end-point suggests that post-annealing resolution may be determined primarily by the annealing conditions. *Escherichia coli* pyrophosphatase crystals annealed in their cryosolution at room temperature also show a post-annealing resolution approximately independent of initial resolution (Samygina *et al.*, 2000).

Fig. 4 shows results of preliminary exploration of how resolution evolves with total annealing time at T = 250 and 230 K, including data for a poorly frozen crystal. At both temperatures, resolution improves in the first $\sim$30 s and is then approximately constant or degrades gradually with longer anneals. The best final resolutions were observed at T = 230 K, although this result is not statistically significant given the limited data. Each data set in Fig. 4 was obtained by performing successive anneals on a single crystal rather than by annealing different crystals for different times; resolution improvements may thus have been limited by the effects of repeated temperature cycling. Single anneals performed at $T \simeq 268$ K rapidly degraded diffraction quality for annealing times beyond $\sim$10 s.

Fig. 5 shows θ–2θ scans for a tetragonal crystal before and after annealing at T = 250 K for 20 s. Annealing typically narrowed the 2θ FWHM by a factor of two and reduced peak structure and the widths of the tails, implying that lattice strain was greatly reduced. The mosaic width sometimes narrowed by $\sim$0.2°, but many crystals showed little mosaic width change despite significantly improved resolution and 2θ width. This may result because of the relatively large post-cooling mosaic widths and because annealing under the conditions explored is largely a local process: annealing a powder at temperatures well below its melting point usually does not change the

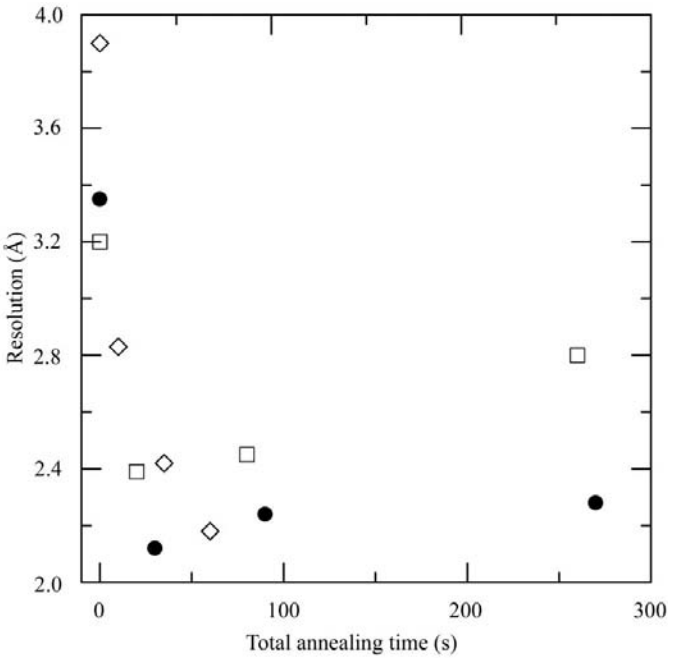

Figure 4
Resolution at I/σ = 8 against annealing time for tetragonal lysozyme crystals annealed at 250 (open symbols) and 230 K (filled symbol).

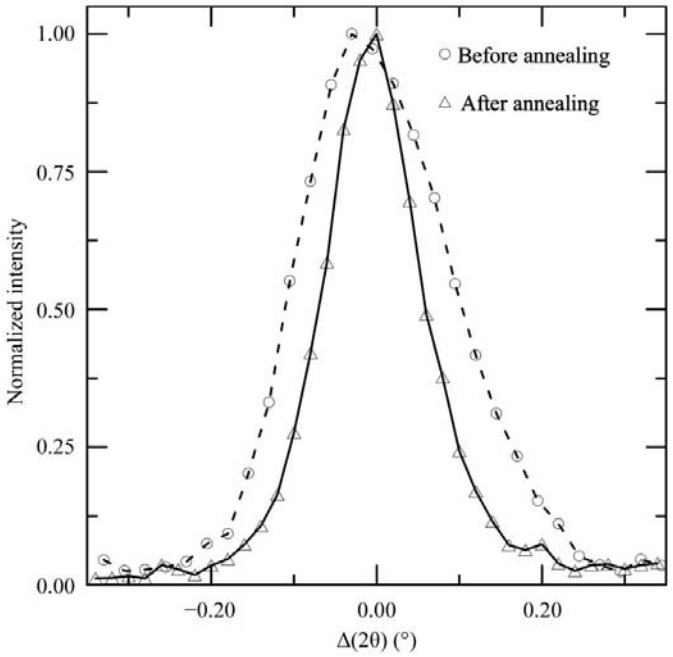

Figure 5
ω–2θ scans for a gel-grown tetragonal lysozyme crystal at $2\theta \simeq 12°$ acquired before and after annealing. The corresponding peak FWHM values are 0.20 and 0.12°.

overall distribution of grain orientations but only the average grain size.

X-ray images provide insight into annealing-induced structural changes that occur within each crystal. As shown in Figs. 1(*e*) and 1(*f*), annealed crystals exhibit a clear mosaic domain structure with a characteristic domain size of ∼20 µm. This domain structure is most pronounced and appears to have a larger characteristic length in crystals having the best final diffraction properties. Fig. 6 shows a sequence of images of an annealed crystal taken at successive angles in the rocking curve of the reflection used for the image. Careful inspection shows that the rocking widths of the individual mosaic domains (<0.5°) are smaller than the overall rocking width of the crystal.

Our results indicate that flash-cooled tetragonal lysozyme crystals are left in a more-or-less uniformly disordered state with a small characteristic length scale for mosaic disorder (*i.e.* a small 'domain' size). Annealing produces larger relatively well ordered domains, each with improved diffraction resolution and mosaicity and reduced strain. These domains have different orientations and the spread in their orientations can be comparable to the crystal's pre-annealing mosaic spread. Fig. 7 illustrates the difference in mosaic character between pre- and post-annealing crystals.

Our experiments using the flash-annealing protocol yielded far less consistent results, with some crystals improving significantly and others degrading. The best final resolution obtained was 1.8 Å and degradation was especially common for crystals that were annealed more than once. This irreproducibility results from rapid sample-dependent warming when the cold stream is blocked and the difficulty of visually identifying when the crystal has reached some target state. While greater experimental skill may have yielded more consistent results, temperature-controlled annealing at $T \leq 250$ K is more robust and routinely provides large improvements for crystals that have suffered significant flash-cooling damage.

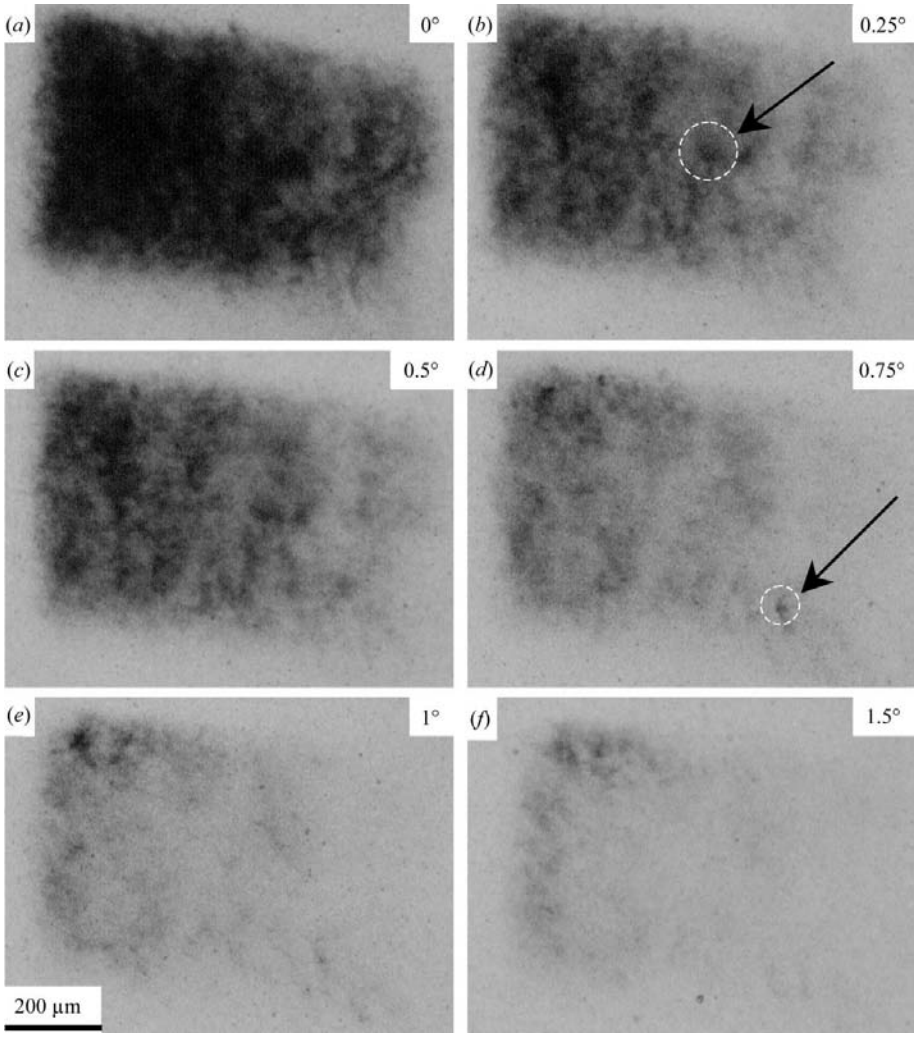

Figure 6
X-ray images of a flash-cooled gel-grown tetragonal lysozyme crystal that has been annealed at 250 K for 30 s, acquired at successive angles in the rocking curve of the reflection used to form the image. Annealing improved the resolution at $I/\sigma = 8$ from 2.9 to 2.4 Å. Two different domains are indicated by arrows in (*b*) and (*d*). Each domain has a mosaic width of ∼0.3° but a different average orientation, producing an overall crystal mosaic width of ∼1°.

3.3. Triclinic lysozyme: flash-cooling and annealing

We also have investigated the effects of flash-cooling and annealing on triclinic HEWL crystals. Consistent with previous observations, the triclinic form survives flash-cooling much better than the tetragonal form, with typical diffraction resolutions of ∼1.7–2 Å at $I/\sigma = 8$. As shown in Fig. 8, X-ray images of flash-cooled unannealed triclinic crystals show large well ordered domains similar to but more pronounced than those we observed in annealed tetragonal crystals. Annealing triclinic crystals at 250 K or by using the flash-annealing technique produced only small changes in diffraction resolution.

4. Discussion

Flash-cooling creates far more disorder in protein crystals than in small-molecule or inorganic crystals. The disorder is also more pervasive: it can include not only cracking and dislocations that degrade mosaicity but, as indicated by degraded resolutions, *B* factors and overall diffracted intensities in crystals that flash-cool poorly, significant disruption of short-range lattice order as well. How does this disorder arise?

4.1. Slow *versus* fast cooling: crystalline *versus* amorphous ice

Macromolecular crystals typically contain between 20 and 90%(*w*/*w*) water. If cooled slowly, this water undergoes a 9% specific volume change as it transforms from its liquid to hexagonal ice phases near $T = 273$ K. The resulting stresses exerted on the protein lattice degrade crystal and diffraction quality. Better diffraction results are obtained when crystals are flash-cooled to temperatures below water's bulk glass transition at $T_g \simeq 140$ K by immersion in a liquid cryogen (nitrogen or propane) or by insertion into a cold stream of gas (nitrogen or helium). Characteristic cooling times, limited by the crystal's thermal conductivity and heat capacity and by heat transfer to the surrounding medium, are estimated to be ~0.1–1 s (Teng & Moffat, 1998; Walker *et al.*, 1998) and are long compared with important microscopic timescales in bulk water (Angell & Choi, 1986).

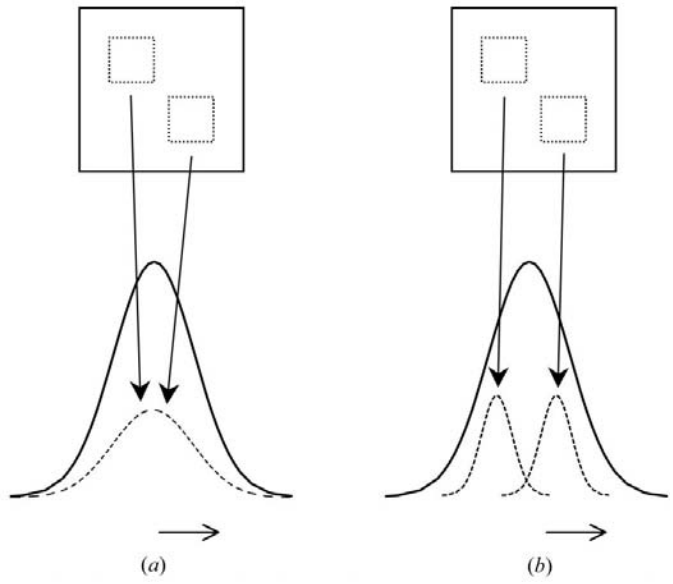

Figure 7
Schematic representation of the character of mosaicity in a flash-cooled tetragonal lysozyme crystal (*a*) before and (*b*) after annealing. In (*a*), each small region of the crystal has a mosaic width comparable to that of the whole crystal. In (*b*), small regions have relatively small mosaic widths but different average orientations, producing a broad overall mosaic width.

By cooling sufficiently rapidly, the transition between liquid water and hexagonal ice (and its abrupt specific volume change) can be bypassed and water can be directly cooled into an amorphous (glassy or microcrystalline) phase. In pure bulk water, vitrification has only been achieved using droplets smaller than 10 µm and cooling rates of $\sim 10^6$ K s^{-1} (Mayer, 1985, 1988). Large protein concentrations dramatically reduce required cooling rates (Sartor *et al.*, 1992, 1994, 1995; Sartor & Mayer, 1994; Peyrard, 2001). For hydrated lysozyme powders with water contents between 23%(*w*/total *w*) (roughly corresponding to the first hydration shell) and 38%(*w*/*w*) (near that required to complete the second hydration shell), cooling rates required to eliminate ice diffraction rings are less than ~4 K s^{-1}, much smaller than typical protein crystal flash-cooling rates of ~200 to 2000 K s^{-1}. Between 38 and 41%(*w*/*w*) water, cooling rates jump by roughly a factor of six and much larger cooling rates are required to freeze additional water layers in more hydrated protein.

To reduce further the cooling rates required to minimize crystalline ice formation, macromolecular crystals are often grown or soaked in cryoprotectants including glycerol, MPD, DMSO, PEGs, alcohols and salts (Hope, 1988, 1990; Mitchell & Garman, 1994; Rodgers, 1994; Garman & Mitchell, 1996; Hey & MacFarlane, 1996, 1998; Garman & Schneider, 1997; Garman, 1999; Rubinson *et al.*, 2000). These may increase solution viscosity, slow hexagonal ice formation and depress its homogeneous nucleation temperature. However, penetrating cryoprotectants like glycerol change other physical and chemical parameters of the solvent that can affect molecular conformation, lattice parameters and crystal stability and can lead to crystal cracking and degradation of diffraction properties even before flash-cooling.

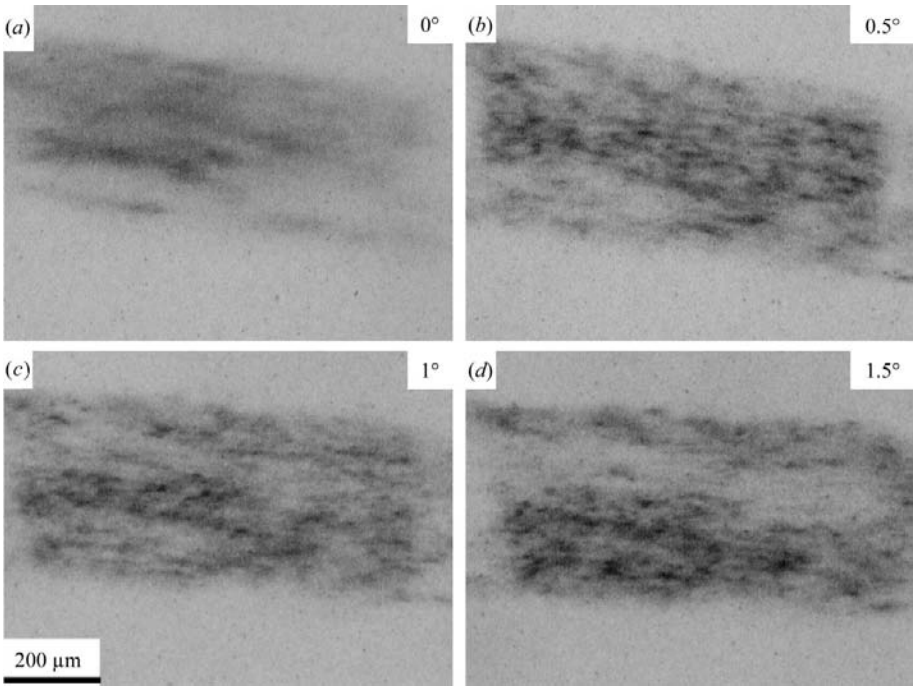

Figure 8
Sequence of X-ray images for a flash-cooled triclinic HEWL crystal, acquired at successive angles in the rocking curve of the reflection used for imaging.

4.2. What happens to water during flash-cooling?

Flash-cooling eliminates the large specific volume change associated with

the phase transition from water to hexagonal ice. So why do crystal diffraction properties still degrade so much? Macromolecular crystallography papers make the implicit or explicit (Weik *et al.*, 2001) assumption that the amorphous form of water produced by flash-cooling has roughly the same density at T = 100 K as liquid water near room temperature, so that there are no stresses associated with its thermal expansion.

This assumption is inconsistent with the behavior of pure bulk water. At ambient pressure and temperatures between 150 and 30 K, water freezes into a low-density amorphous ice phase (Ghormley & Hochanadel, 1971; Mayer, 1994; Westley *et al.*, 1998). Amorphous ice expands when cooled and at 77 K has a density of 0.94 g cm^{-3}. This is very close to the density of hexagonal ice at this temperature (Röttger *et al.*, 1994), which contracts on cooling below T = 273 K. In both crystalline and amorphous forms, water tries to maximize its hydrogen bonding on cooling, leading to a tetrahedral coordination of water molecules. Differences in the structure of the crystalline and amorphous forms are a consequence of small variations in the bond angles and bond lengths of the tetrahedra (Dore, 1985; Elliott, 1995); in the presence of salts and cryoprotectants these differences are likely to be even smaller. Although water in the protein's first hydration shell, which has many of its hydrogen bonds satisfied by the protein, may have its structure and, therefore, density altered from that of bulk amorphous water (Chen *et al.*, 1995; Wiggins, 1995; Bellissent-Funel, 1998; Dellerue & Bellissent-Funel, 2000), the remaining crystal water should show bulk-like behavior, consistent with calorimetry studies (Miyazaki *et al.*, 2000). Consequently, flash-cooling should produce nearly as large an increase in water's specific volume between room temperature and T = 100 K as slow-cooling into the hexagonal ice phase.

4.3. But don't protein crystals shrink during flash-cooling?

The lattice parameters of macromolecular crystals decrease when the crystals are flash-cooled. Between T = 293 and T = 100 K, the lattice constants typically change by ∼1–3% and the unit-cell volume by ∼3–6% (Frauenfelder *et al.*, 1987; Earnest *et al.*, 1991; Young *et al.*, 1994; Kurinov & Harrison, 1995; Watowich *et al.*, 1995; Weik *et al.*, 2001). The probe-accessible volume deduced from electron-density maps also shrinks by ∼1–2% on cooling. How can this lattice contraction be consistent with a large expansion of the crystal water, especially in crystals with water contents of 50% or more?

This apparent paradox may be resolved by recognizing that flash-cooled macromolecular crystals are really composite materials consisting of interpenetrating protein and solvent structures and that X-ray diffraction only probes the average thermal expansion behavior of the ordered protein structure. The protein and solvent components in general will have their own thermal expansion behavior and the overall thermal expansion of the composite may be roughly a weighted sum of the expansions of these components. Consequently, if the water content is large enough and the concentration of water-structure-disrupting additives such as salts is small enough, the crystal may expand even though the protein lattice contracts.

4.4. Protein lattice contraction and water expansion: an explanation for low-temperature crystal microstructure?

As in any other composite material, differential thermal expansion of the protein and solvent/amorphous ice components should have important consequences for crystal microstructure. If the protein lattice contracts and the probe-accessible volume shrinks during flash-cooling, then where does the expanding water go? Were the crystal cooled very slowly, water would eventually be squeezed out and accumulate at its surface. But when crystals are flash-cooled, such large-scale movements are not possible in the ∼0.1–1 s before the water vitrifies. These timescales are sufficient for more short-range redistributions of water.

We suggest that during flash-cooling, water is expelled from small grains within the crystal and accumulates in water-rich regions surrounding each grain. The protein lattice within the grains may be well ordered and produce the sharp peaks with

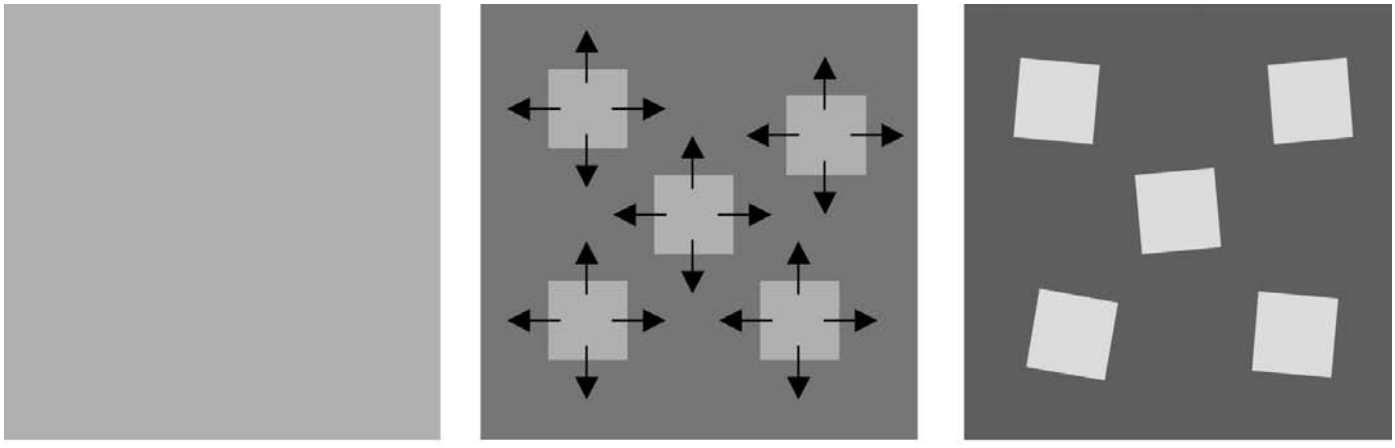

Figure 9
Schematic illustration of protein crystal microstructure (*a*) before, (*b*) during and (*c*) after flash-cooling. The shading density indicates local water concentration.

reduced lattice constants observed in low-temperature diffraction. However, the surrounding water-rich regions become disrupted, reducing the ordered fraction of the crystal and thus overall diffraction intensities and resolution. Stresses associated with this microheterogeneity cause rotations of the ordered protein grains that broaden the mosaicity. This mechanism is illustrated in Fig. 9 and the result is a classic mosaic crystal. This crystal microstructure is consistent with that observed for flash-cooled triclinic lysozyme crystals in Fig. 8, which contrasts with the featureless topographs of as-grown lysozyme crystals in Figs. 2(*a*) and 2(*b*).

The size of the grains and overall lattice order should depend on many factors including cooling kinetics, crystal solvent content and solvent composition (which determines its expansion behavior). With increasing internal cooling rates, the size of the disordering solvent redistribution should decrease so that diffraction properties may improve. With increasing solvent content beyond that required for protein hydration, the amount of water that must be expelled to disordered regions between grains increases. For similar flash-cooling conditions, more solvent-rich crystal forms may develop smaller ordered protein grains and a larger ratio of disordered to ordered protein volume, resulting in a broader mosaic width and poorer diffraction resolution. This is consistent with our results for flash-cooling of tetragonal and triclinic lysozyme: the triclinic form has a lower water content and after flash-cooling consistently diffracts to higher resolution with smaller mosaicity and larger ordered grains. This is also consistent with the general observation that crystals with large solvent contents are more difficult to flash-cool successfully. Poor flash-cooling behavior may also be in part a consequence of the larger cooling rates needed to vitrify the solvent, but solvent-rich crystal forms that do not show appreciable ice-ring intensity often diffract poorly after cooling. These arguments should hold regardless of the solvent composition and solvent thermal expansion behavior, so long as the latter differs from that of the protein lattice.

4.5. An alternative view of the role of cryoprotectants

Cryoprotectants can be broadly grouped into two categories: those that penetrate into the crystal and those that do not. Nonpenetrating cryoprotectants such as oils and large MW PEGs help remove surface water that could freeze and damage the crystal, and prevent surface water from crystallizing on cooling by increasing viscosity and suppressing ice-crystal nucleation. Penetrating cryoprotectants such as glycerol and MPD are used to suppress hexagonal ice nucleation and growth inside the crystal and facilitate the transition of water to the amorphous phase. Review articles on cryoprotection cite equilibrium phase diagrams for bulk water and searches for appropriate cryoprotectants have used protein-free mixtures of water and cryoprotectants (Garman & Mitchell, 1996; Garman & Schneider, 1997).

However, dissolved protein significantly modifies the nucleation and crystallization behavior of ice and the cooling rates required to achieve amorphous ice (Sartor *et al.*, 1992, 1994, 1995; Sartor & Mayer, 1994; Peyrard, 2001). The very high density of protein within protein crystals is itself very effective in suppressing ice nucleation and reducing cooling rates. Aside from large or very high solvent-content crystals, most crystals can be flash-cooled without generating appreciable ice-ring intensity, provided the surrounding solvent is removed or treated with nonpenetrating cryoprotectants.

The discussion of §4.4 suggests another, possibly more important, role for penetrating cryoprotectants: thermal expansion matching. Unlike water, most if not all standard cryoprotectants contract on cooling and have higher densities at 100 K than at room temperature. Consequently, by using appropriate mixtures of water and cryoprotectants it should be possible to match the solvent and protein lattice expansions and thereby dramatically reduce disordering lattice stresses at low temperatures. A similar approach to choosing concentrations of nonpenetrating cryoprotectants should reduce stresses exerted by differential contraction of the surrounding solvent. Thermal expansion matching may also be of use in cryopreservation of tissues.

Are the required cryoprotectant concentrations feasible? For example, tetragonal lysozyme crystals have a water content of ∼42% and the volume of their protein lattice contracts by ∼5% between 293 and 100 K. Estimating the density of flash-cooled glycerol–water mixtures by interpolating between the measured expansions for flash-cooled water (6%) and slow-cooled glycerol (–12.4%), assuming that the glycerol-to-water ratio in the crystal is the same as in the soak solution, and ignoring water inside the first hydration shell, the required glycerol concentration is ∼30%. Perhaps coincidentally, this is the glycerol concentration typically used for flash-cooling tetragonal lysozyme crystals.

An interesting consequence of the above ideas is that the search for 'cryoprotectants' can be broadened. In particular, since penetrating cryoprotectants are not in most cases required to inhibit crystalline ice formation, any protein-friendly fluid or additive that provides expansion matching but no particular benefits for ice crystallization can be explored.

4.6. Homogeneous *versus* inhomogeneous effects

Mosaic broadening and resolution degradation caused by flash-cooling are a consequence in part of processes such as those discussed above that occur more-or-less uniformly throughout the crystal volume. However, in sufficiently large crystals heat transport is limited by the crystal's bulk thermal conductivity. In this regime, large spatial variations of temperature and cooling rate within the crystal should produce transient gradients in protein lattice constant, in solvent specific volume and perhaps also in molecular conformation. The resulting stresses may drive defect formation and mosaic broadening that is inhomogeneous within the crystal, as occurs during crystal dehydration (Dobrianov *et al.*, 2001).

However, numerical estimates based on dimensional arguments to be described in detail elsewhere suggest that heat transport even in very large protein crystals is limited by the

cooling-gas boundary layer, not by transport within the crystal. Temperature differences ΔT between the crystal surface and core should vary with crystal size L as $\Delta T \propto L^{1/2}$; for $L \simeq 1$ mm, $\Delta T \simeq 10$ K and ΔT becomes smaller in smaller crystals. Our X-ray images for millimetre-size crystals show no clear evidence of differences in crystalline order between surface regions and interior regions. This is consistent with small spatial variations of temperature and suggests that disordering processes that occur uniformly on the scale of the crystal are more important in degrading diffraction quality. Section topography should be used to more accurately evaluate differences in order between surface and interior crystal regions.

Scaling arguments also indicate that the characteristic crystal cooling rate $\Delta T/\Delta t \propto L^{-3/2}$ and increases by a factor of $\sim$30 as crystal size L decreases from 1 mm to 100 µm. Size-dependent cooling rates and corresponding variations in, for example, solvent segregation kinetics, water crystallization and protein lattice microstructure are likely to be responsible for increased flash-cooling-induced disorder in larger crystals.

4.7. Origin of ice rings

Ice rings may appear in diffraction patterns owing to crystallization of water inside the crystal, of residual water between the crystal and CryoLoop and of water vapor condensed from the air. This crystallization interferes with measurements of particular reflections, but often has limited effects on diffraction from the protein lattice itself.

Ice rings from condensed vapor are easily distinguished and can be eliminated with proper cryocooling hardware. Ice rings from residual surface water and from internal crystal water are more difficult to distinguish and so penetrating cryoprotectant solutions are often chosen to eliminate all ice-ring diffraction. However, crystallizing internal water is much harder because of the protein's cryoprotective properties. Consequently, penetrating cryoprotectant concentrations that eliminate ice rings may be much larger and more damaging than those needed to prevent ice-crystal growth from internal water, and generally will not provide optimum solvent–protein thermal expansion matching. When possible, crystallization of internal and surface water should be treated and optimized separately using a combination of penetrating and nonpenetrating cryoprotectants and careful surface-liquid removal.

How are ice rings from inside the crystal itself generated? Typical observed ice-ring widths in tetragonal lysoyzme crystals of $\leq 0.3^\circ$ imply crystalline ice correlations on lengths longer than $\sim$200 Å, much larger than the unit-cell size. Correlated crystalline order on $\sim$200 Å scales could develop as crystalline ice grows in interconnected pores and channels of the ideal protein lattice (Weik *et al.*, 2001). This is especially likely in high-solvent-content crystals, where the pore size may be much larger than the $\sim$10 Å over which water's hydrogen bonding is disrupted by interactions with protein surfaces.

Crystallization in water-rich regions of the protein lattice associated with defects like inclusions, vacancies, dislocations and grain boundaries may be even more important. These defects may be produced during growth or by protein lattice contraction and water expulsion during flash-cooling. Lattice defects provide much larger protein-free volumes than intrinsic pores and channels in which ice-crystal nucleation and growth can occur and may 'seed' ice growth in nearby ordered regions of the protein lattice. Observed ice-ring intensities typically correspond to crystallization of only a tiny fraction of the internal water. Defect-related inhomogeneous crystallization may be responsible.

4.8. Mechanism of annealing

When protein crystals are flash-cooled, the distribution of lattice orientations (mosaicity) and spacings increases by one to two orders of magnitude and diffraction resolution degrades. In our experiments, the extent of resolution degradation correlates with the width of the lattice-spacing distribution. Annealing crystals by warming to temperatures of 230–250 K reduces the distribution of lattice spacings and improves diffraction resolution. X-ray topographs (*e.g.* Figs. 2 and 6) indicate that annealing produces larger better ordered domains and reduces the lattice-spacing spread. Annealing of protein crystals thus has some similarities to annealing of inorganic materials, in that cooled-in lattice stresses can drive local lattice reordering and domain growth when the lattice is warmed. At low temperatures solids become brittle, but at higher temperatures dislocation movement and plastic deformations occur more easily. This allows lattice stress to be released and ordered grains to form by defect annihilation and by defect migration to grain boundaries.

The composite nature and weaker bonding interactions of macromolecular crystals adds new features to their annealing and allows it to proceed on timescales of seconds at relatively low temperatures. The large stresses that can develop in flash-cooling owing to differential expansion and inhomogeneous cooling cannot relax because of the rigid scaffolding provided by amorphous solvent. Protein lattice stress release and defect migration can occur when water molecules develop significant mobility, which occurs well below water's freezing point. The Young's modulus of tetragonal lysozyme shows a sixfold decrease as the crystals are warmed from 150 to 240 K and an abrupt drop at $\sim$243 K attributed to melting of a fraction of the intracrystalline water (Morozov & Gevorkian, 1985). Large salt concentrations present in many protein crystals [*e.g.* between 2 and 25%(*w*/*w*) of protein in tetragonal lysozyme grown using NaCl] also can promote low-temperature melting.

The effectiveness of annealing at temperatures well below the freezing point of bulk water may also be related to the general phenomenon of interfacial melting (Dash *et al.*, 1995; Wettlaufer & Dash, 2000). The melting point of water at surfaces, of ice (Dosch *et al.*, 1995; Wettlaufer & Dash, 2000), diverse granular media (Maruyama *et al.*, 1992) and porous glasses (Ishizaki *et al.*, 1996), is suppressed to temperatures typically approaching 253 K, with the thickness of the fluid interfacial layer increasing with temperature from a few monolayers at 243 K. In the tightly confined large-curvature interstices of protein crystals, interfacial melting may allow

increased mobility and relaxation of the protein lattice in this temperature range and perhaps below it.

4.9. Why does annealing eventually degrade crystal diffraction?

Our very limited experiments suggest that annealing degrades diffraction quality after an annealing time that decreases with increasing temperature. This degradation may in part arise from temperature-dependent changes in protein conformation. Likely to be more important is growth of lattice-disrupting cubic or hexagonal ice, which begins at temperatures above the glass transition $T_g \simeq 140$ K (Weik *et al.*, 2001). As discussed in §4.7, ice-crystal growth may occur in water-rich regions produced by growth defects or by defects created during flash-cooling. Protein lattice stresses and ordinary ice-crystal growth processes may also drive consolidation of water into larger ice grains. Ice crystallization effects should be reduced by matching the solvent and protein lattice thermal expansions.

Protein crystals may also be subject to thermally driven ice segregation and 'frost heave' (Dash, 1989, 1992). In granular media such as soils, temperature gradients produce a thermomolecular pressure that drives motion of liquid water at temperatures that, because of interfacial melting, extend well below the bulk solid–liquid boundary. Water flows through interfacial layers from warmer regions to colder regions, where it can continue to accumulate between grains until the water pressure becomes large enough counteract the thermomolecular pressure. The thermomolecular pressure is independent of the soil's physical and chemical nature and depends only on temperature profiles and the thermodynamic properties of ice. This pressure causes soils to rupture and water then flows and freezes, forming ice layers that separate the soil and heave the ground above. With their easily disrupted lattices, protein crystals may be subject to similar effects well above water's glass-transition temperature, and the resulting ice crystals may contribute to the narrowing and coarsening of their ice rings.

Minimizing 'frost heave' during protein crystal annealing may thus require minimizing temperature fluctuations in the cold stream and resulting temperature gradients within the crystal. Diffraction degradation and ice-ring growth observed when early cryocoolers were used for long data-collection runs may have arisen in part from frost-heave effects, since early coolers provided relatively poor temperature stability and operated at temperatures above T_g. Modern cryocoolers provide excellent stability, but their lower cooling temperatures and the much shorter data-collection times (<1 h) made possible by intense synchrotron sources may have made their improved stability irrelevant.

4.10. Mechanisms of 'macromolecular crystal annealing' and 'flash-annealing'

In flash-annealing (Yeh & Hol, 1998), crystals are warmed for a few seconds by blocking the cold stream. Improvements in crystal quality should occur by the same mechanisms as in the constant-temperature annealing that we have been exploring. However, our approach should be more reproducible and flexible because of the more precise control over annealing temperature and time.

In 'macromolecular crystal annealing' (Harp *et al.*, 1998, 1999), flash-cooled crystals are returned to their original cryoprotectant solution, soaked for 3 min and are then flash-cooled a second time. How does this annealing method improve crystal diffraction, given that similar temperature gradients and protein–solvent segregation effects should occur during both the first and second flash-coolings?

During the first cooling the protein lattice develops grains separated by highly defected regions. At room temperature, protein molecules have large mobilities near lattice defects. Dislocations, cracks and other disorder produced during heavy-atom soaks or dehydration, for example, can spontaneously heal, sometimes producing nearly complete recovery of diffraction properties (for example, see Dobrianov *et al.*, 2001). The room-temperature soaks of macromolecular crystal annealing are likely to allow short-scale disorder produced by flash-cooling to anneal into larger ordered grains separated by disordered grain boundaries, as occurs during annealing at lower temperatures. These grain boundaries are mechanically weak and during the second flash-cooling they may provide natural places for plastic slip, stress release and water expulsion, leaving the interior of the ordered grains more or less intact. Since crystal B factors are largely determined by short-length-scale ordering and (unlike mosaicity) are only weakly affected by the presence of grains at micrometre or larger scales, order developed by grain growth during the anneal may improve the low-temperature resolution.

'Macromolecular crystal annealing' is obviously a special case of the fixed-temperature annealing studied here, although the mechanisms of annealing above and below the bulk-solvent melting point differs in important ways. Expanding the range of annealing temperatures expands the phase space for optimization.

4.11. Annealing and radiation damage

Warming crystals during annealing may increase radiation damage by allowing radicals generated during previous low-temperature X-ray exposure to diffuse and react and by allowing molecular and lattice relaxation in response to this chemical damage. Experiments on macromolecules in solution (Dertinger & Jung, 1970) indicate that cooling from room temperature to 100 K reduces radiation damage by roughly three orders of magnitude and that two orders of magnitude of this reduction occur when water solidifies at 273 K. Consequently, fixed-temperature anneals at temperatures where the solvent remains solid may be necessary for crystals that have received significant radiation doses.

5. Conclusions

The present results help to establish the nature of macromolecular crystal disorder induced by flash-cooling and how

annealing can reduce this disorder. They provide evidence that differential thermal expansion of macromolecular crystal components during flash-freezing is the dominant source of this disorder, with potentially important consequences for choice of cryoprotectants. We also have demonstrated an alternative annealing protocol requiring warming to temperatures well below the bulk-solvent melting point. This protocol is easy to implement and provides large and highly reproducible improvements in diffraction quality of more disordered crystals.

Annealing provides the largest diffraction-quality improvements for crystals that suffer the most damage on cooling, while crystals that before annealing diffract to the highest resolution seem to benefit little. Consequently, annealing is likely to be most important for obtaining useful structural information before cryoprotectants and cooling procedures have been fully optimized and for macromolecules that are too scarce to allow such optimization.

Further optimization of annealing protocols will involve balancing disorder reduction through strain release and domain growth with disorder increase arising from water crystallization and protein conformation changes. The experimental techniques used here, especially X-ray topography and ω–2θ lineshape measurements, should play an important role in further development of flash-cooling and annealing protocols.

A recent article (Juers & Matthews, 2001) has also suggested that differential expansion of the protein lattice and crystal solvent may be an important contributor to flash-cooling-induced disorder. Reported density data for flash-cooled solvents together with lattice thermal contraction and repacking data for β-galactosidase support the existence of differential expansion and the use of cryoprotectants to reduce it.

We wish to thank A. A. Chernov, R. Headrick, A. Deacon, D. Tolbert and S. Ealick for fruitful discussions, and A. Kisselev, M. Brink and H.-P. Goh for technical assistance. This work is supported by NASA (NAG8-1357 and NAG8-1831). CHESS is supported by the National Science Foundation and the National Institutes of Health/National Institute of General Medical Sciences under award DMR 9713424.

References

Angell, C. A. & Choi, Y. (1986). *J. Microsc.* **141**, 251–261.
Bellissent-Funel, M. C. (1998). *J. Mol. Liq.* **78**, 19–28.
Caylor, C. L., Dobrianov, I., Lemay, S. G., Kimmer, C., Kriminski, S., Finkelstein, K. D., Zipfel, W., Webb, W. W., Thomas, B. R., Chernov, A. A. & Thorne, R. E. (1999). *Proteins*, **36**, 270–281.
Chayen, N. E., Boggon, T. J., Cassetta, A., Deacon, A., Gleichmann, T., Habash, J., Harrop, S. J., Helliwell, J. R., Nieh, Y. P., Peterson, M. R., Raftery, J., Snell, E. H., Hadener, A., Niemann, A. C., Siddons, D. P., Stojanoff, V., Thompson, A. W., Ursby, T. & Wulff, M. (1996). *Q. Rev. Biophys.* **29**, 227–278.
Chen, S. H., Gallo, P. & Bellissent-Funel, M.-C. (1995). *Can. J. Phys.* **73**, 703–709.
Dash, J. G. (1989). *Contemp. Phys.* **30**, 89–100.
Dash, J. G. (1992). *J. Low-Temp. Phys.* **89**, 277–285.
Dash, J. G., Fu, H. Y. & Wettlaufer, J. S. (1995). *Rep. Prog. Phys.* **58**, 115–167.
Dellerue, S. & Bellissent-Funel, M. C. (2000). *Chem. Phys.* **258**, 315–325.
Dertinger, H. & Jung, H. (1970). *Molecular Radiation Biology: the Action of Ionizing Radiation on Elementary Biological Objects.* New York: Springer–Verlag.
Dobrianov, I., Caylor, C., Lemay, S. G., Finkelstein, K. D. & Thorne, R. E. (1999). *J. Cryst. Growth*, **196**, 511–523.
Dobrianov, I., Finkelstein, K. D., Lemay, S. G. & Thorne, R. E. (1998). *Acta Cryst.* D**54**, 922–937.
Dobrianov, I., Kriminski, S., Caylor, C. L., Lemay, S. G., Kimmer, C., Kisselev, A., Finkelstein, K. D. & Thorne, R. E. (2001). *Acta Cryst.* D**57**, 61–68.
Dore, J. C. (1985). *Water Sci. Rev.* **1**, 3–92.
Dosch, H., Lied, A. & Bilgram, J. H. (1995). *Surf. Sci.* **327**, 145–164.
Earnest, T., Fauman, E., Craik, C. S. & Stroud, R. (1991). *Proteins*, **10**, 171–187.
Elliott, S. R. (1995). *J. Chem. Phys.* **103**, 2758–2761.
Fourme, R., Ducruix, A., Ries-Kautt, M. & Capelle, B. (1995). *J. Synchrotron Rad.* **2**, 136–142.
Frauenfelder, H., Hartmann, H., Karplus, M., Kuntz, I. D., Kuriyan, J., Parak, F., Petsko, G. A., Ringe, D., Tilton, R. F., Connolly, M. L. & Max, N. (1987). *Biochemistry*, **26**, 254–261.
Garman, E. (1999). *Acta Cryst.* D**55**, 1641–1653.
Garman, E. F. & Mitchell, E. P. (1996). *J. Appl. Cryst.* **29**, 584–587.
Garman, E. F. & Schneider, T. R. (1997). *J. Appl. Cryst.* **30**, 211–237.
Ghormley, J. A. & Hochanadel, C. J. (1971). *Science*, **171**, 62–64.
Harp, J. M., Hanson, B. L., Timm, D. E. & Bunick, G. J. (1999). *Acta Cryst.* D**55**, 1329–1334.
Harp, J. M., Timm, D. E. & Bunick, G. J. (1998). *Acta Cryst.* D**54**, 622–628.
Hey, J. M. & MacFarlane, D. R. (1996). *Cryobiology*, **33**, 205–216.
Hey, J. M. & MacFarlane, D. R. (1998). *Cryobiology*, **37**, 119–130.
Hope, H. (1988). *Acta Cryst.* B**44**, 22–26.
Hope, H. (1990). *Annu. Rev. Biophys. Biophys. Chem.* **19**, 107–126.
Ishizaki, T., Maruyama, M., Furukawa, Y. & Dash, J. G. (1996). *J. Cryst. Growth*, **163**, 455–460.
Izumi, K., Sawamura, S. & Ataka, M. (1996). *J. Cryst. Growth*, **168**, 106–111.
Juers, D. H. & Matthews, B. W. (2001). *J. Mol. Biol.* **311**, 851–862.
Kurinov, I. V. & Harrison, R. W. (1995). *Acta Cryst.* D**51**, 98–109.
Maruyama, M., Bienfait, M., Dash, J. G. & Coddens, G. (1992). *J. Cryst. Growth*, **118**, 33–40.
Mayer, E. (1985). *J. Microsc.* **140**, 3–15.
Mayer, E. (1988). *Cryo-Lett.* **9**, 66–77.
Mayer, E. (1994). In *Hydrogen-Bonded Networks*, edited by M. C. Bellissent-Funel & J. C. Dore. Dordrecht: Kluwer.
Mitchell, E. P. & Garman, E. F. (1994). *J. Appl. Cryst.* **27**, 1069–1074.
Miyazaki, Y., Matsuo, T. & Suga, H. (2000). *J. Phys. Chem. B*, **104**, 8044–8052.
Morozov, V. N. & Gevorkian, S. G. (1985). *Biopolymers*, **24**, 1785–1799.
Nave, C. (1998). *Acta Cryst.* D**54**, 848–853.
Nave, C. (1999). *Acta Cryst.* D**55**, 1663–1668.
Otalora, F., Garcia-Ruiz, J. M., Gavira, J.-A. & Capelle, B. (1999). *J. Cryst. Growth*, **196**, 546–558.
Parkin, S. & Hope, H. (1998). *J. Appl. Cryst.* **31**, 945–953.
Peyrard, M. (2001). *Phys. Rev. E*, **64**, 011109.
Rodgers, D. W. (1994). *Structure*, **2**, 1135–1140.
Röttger, K., Endriss, A., Ihringer, J., Doyle, S. & Kuhs, W. F. (1994). *Acta Cryst.* B**50**, 644–648.
Rubinson, K. A., Ladner, J. E., Tordova, M. & Gilliland, G. L. (2000). *Acta Cryst.* D**56**, 996–1001.
Samygina, V. R., Antonyuk, S. V., Lamzin, V. S. & Popov, A. N. (2000). *Acta Cryst.* D**56**, 595–603.
Sartor, G., Hallbrucker, A., Hofer, K. & Mayer, E. (1992). *J. Phys. Chem.* **96**, 5133–5138.

Sartor, G., Hallbrucker, A. & Mayer, E. (1995). *Biophys. J.* **69**, 2679–2694.
Sartor, G. & Mayer, E. (1994). *Biophys. J.* **67**, 1724–1732.
Sartor, G., Mayer, E. & Johari, G. P. (1994). *Biophys. J.* **66**, 249–258.
Singh, T. P., Bode, W. & Huber, R. (1980). *Acta Cryst.* B**36**, 621–627.
Stojanoff, V. & Siddons, D. P. (1996). *Acta Cryst.* A**52**, 498–499.
Tanner, B. K. (1976). *X-ray Diffraction Topography*. Oxford/New York: Pergamon Press.
Teng, T. Y. & Moffat, K. (1998). *J. Appl. Cryst.* **31**, 252–257.
Vidal, O., Robert, M.-C., Capelle, B. & Arnoux, B. (1999). *J. Cryst. Growth*, **196**, 559–571.
Walker, L. J., Moreno, P. O. & Hope, H. (1998). *J. Appl. Cryst.* **31**, 954–956.
Watowich, S. J., Skehel, J. J. & Wiley, D. C. (1995). *Acta Cryst.* D**51**, 7–12.
Weik, M., Kryger, G., Schreurs, A. M. M., Bouma, B., Silman, I., Sussman, J. L., Gros, P. & Kroon, J. (2001). *Acta Cryst.* D**57**, 566–573.
Westley, M. S., Baratta, G. A. & Baragiola, R. A. (1998). *J. Chem. Phys.* **108**, 3321–3326.
Wettlaufer, J. S. & Dash, J. G. (2000). *Sci. Am.* **282**, 50–53.
Wiggins, P. M. (1995). *Prog. Polym. Sci.* **20**, 1121–1163.
Yeh, J. I. & Hol, W. G. J. (1998). *Acta Cryst.* D**54**, 479–480.
Young, A. C. M., Dewan, J. C., Nave, C. & Tilton, R. F. (1993). *J. Appl. Cryst.* **26**, 309–319.
Young, A. C. M., Tilton, R. F. & Dewan, J. C. (1994). *J. Mol. Biol.* **235**, 302–317.